

# Dimer-vacancy reconstructions of the GaN and ZnO(10 $\bar{1}$ 1) surfaces: Density functional theory calculations

Woo-Jin Lee and Yong-Sung Kim\*

*Korea Research Institute of Standards and Science, Yuseong, Daejeon 305-340, Korea*

(Received 12 July 2011; revised manuscript received 3 August 2011; published 22 September 2011)

Reconstructed structures of the GaN and ZnO(10 $\bar{1}$ 1) anion semipolar surfaces were studied using density functional theory calculations. The twofold-coordinated anion atoms on the unreconstructed surfaces form anion dimers with reduced surface hole density. The residual holes on the dimerized surfaces are additionally compensated by formation of a dimer vacancy (DV) in every four  $2 \times 1$  cells on GaN(10 $\bar{1}$ 1) and in two  $2 \times 1$  cells on ZnO(10 $\bar{1}$ 1). The electrostatically stable  $4 \times 2$  DV reconstruction on the GaN(10 $\bar{1}$ 1) surface is found to be more stable than the previously suggested structures, and the  $2 \times 2$  DV reconstruction on the ZnO(10 $\bar{1}$ 1) surface explains the transmission electron microscopy observations.

DOI: [10.1103/PhysRevB.84.115318](https://doi.org/10.1103/PhysRevB.84.115318)

PACS number(s): 68.35.bg

## I. INTRODUCTION

GaN and ZnO semiconductors are important for optoelectronic device applications. The GaN thin films, typically grown in the [0001] direction, have dense dislocations. In order to reduce polarization effects, the nonpolar or semipolar growth of GaN thin films has been studied intensively.<sup>1-5</sup> Meanwhile, the {10 $\bar{1}$ 1} semipolar surfaces have been observed, commonly at the facets of hexagonal pyramid nanostructures<sup>6-9</sup> and inverted-pyramid-shaped dislocation pits on GaN thin films (V defects).<sup>10,11</sup> To understand and control the epitaxial growth of thin films and nanostructures, we need to know the surface atomic structures. In spite of the technological importance and the natural abundance of the (10 $\bar{1}$ 1) surface, the reconstructed structures still remain unclear.

On conventional semiconductor surfaces, the structures of the surface reconstructions are explained by a small number of guiding principles.<sup>12-14</sup> (i) First, surfaces tend to reduce the number of dangling bonds (e.g., by forming dimers). (ii) Second, surfaces minimize their electronic energy by satisfying the electron counting rule. (iii) Finally, they tend to minimize the electrostatic energy by optimizing the arrangement of the charged surface atoms or vacancies. On the GaN(0001) surface, in N-rich conditions, the stable  $2 \times 2$  N adatom (*H3*) structure is semiconducting and satisfies the general rules.<sup>15-19</sup> The stable  $2 \times 2$  Ga adatom (*H3*) structure in N-rich conditions on the GaN(000 $\bar{1}$ ) surface is also semiconducting and follows the rules.<sup>15,16</sup> While the surfaces are semiconducting in N-rich conditions, they tend to be metallic in Ga-rich conditions because they are reconstructed to the Ga-bilayer [GaN(0001)] or Ga-adlayer [GaN(000 $\bar{1}$ )] structures.<sup>15,17,19,20</sup> On the GaN(10 $\bar{1}$ 1) N-semipolar surface, the Ga-adlayer structure in Ga-rich conditions is very similar to that on the GaN(000 $\bar{1}$ ) N-polar surface.<sup>21,22</sup> However, in N-rich conditions, the previously suggested  $1 \times 1$  Ga adatom (*H3*) and  $1 \times 1$  N-vacancy structures on the GaN(10 $\bar{1}$ 1) surface are dissimilar to the semiconducting reconstructed structure of the GaN(000 $\bar{1}$ ) N-polar surface and have 0.75 free electrons per an  $1 \times 1$  unit cell, violating the electron counting rule.<sup>21,22</sup> For ZnO, the surface reconstructions have not been studied extensively. On the ZnO(10 $\bar{1}$ 1) O-semipolar surface, the  $a \times 2$  reconstruction has been reported based on a transmission electron microscopy (TEM)

experiment,<sup>23</sup> but the detailed atomic structures remain to be elucidated.

In this paper, we report the  $4 \times 2$  dimer-vacancy (DV) and  $2 \times 2$  DV reconstructions on the GaN and ZnO(10 $\bar{1}$ 1) surfaces, respectively, following the general reconstruction rules of semiconductor surfaces. The structures of the reconstructions are semiconducting and found to be the most stable in anion-rich conditions in density functional theory (DFT) calculations. The reconstructions of the pristine GaN and ZnO surfaces are only focused on in relation to the molecular beam epitaxial (MBE) growth. For metal organic vapor-phase epitaxy (MOVPE), the adsorbates such as hydrogen can affect the structures of the surface reconstructions.

## II. CALCULATIONAL METHOD

The DFT calculations were performed as implemented in the Vienna *ab initio* simulation package (VASP) code.<sup>24</sup> The projector-augmented-wave (PAW) pseudopotentials and the plane-wave basis set with a kinetic cutoff energy of 400 eV were used.<sup>25</sup> The Ga and Zn *3d* electrons were included in the valence state. For exchange correlation energy, the generalized gradient approximation (GGA) was used,<sup>26</sup> and the onsite Coulomb energy correction (*U*) of 6 eV was applied to the Zn *3d* states for ZnO.<sup>27</sup>

The periodic slab structures were used for the GaN and ZnO(10 $\bar{1}$ 1) surface models. For the  $1 \times 1$ ,  $2 \times 1$ ,  $2 \times 2$ , and  $4 \times 1$  reconstructions, we used thick slabs: the 10-GaN(ZnO)-bilayer-thick ( $\sim 22$ -Å) slab. For the larger unit-cell reconstructions, we used thinner slabs because of the large number of atoms in the supercell. For the  $6 \times 2$ ,  $2 \times 6$ ,  $12 \times 1$ ,  $4 \times 3$ ,  $2 \times 4$ ,  $4 \times 2$ , and  $8 \times 1$  reconstructions on GaN(10 $\bar{1}$ 1), we used the 5-GaN-bilayer-thick ( $\sim 11$ -Å) slabs. For the  $4 \times 2$  reconstructions on ZnO(10 $\bar{1}$ 1), we used the 5-ZnO-bilayer-thick ( $\sim 10$ -Å) slab. The surface energy differences between the thick and thin slabs for various  $1 \times 1$ ,  $2 \times 1$ , and  $2 \times 2$  reconstructions were checked and found to be less than 10 meV/( $1 \times 1$ ). The vacuum space between slabs is about 10 Å for all cases. The bottom surface of the slabs is passivated by pseudohydrogen to make the surface charge neutral. The bottom two GaN(ZnO) bilayers were fixed to mimic the bulk, and the Hellmann-Feynman forces were relaxed less than

0.02 eV/Å. The theoretical lattice constants were used:  $a = 3.215$  Å and  $c/a = 1.627$  for GaN and  $a = 3.212$  Å and  $c/a = 1.614$  for ZnO. The  $k$ -point set equivalent to the  $6 \times 4$  mesh in the  $1 \times 1$  surface Brillouin zone was mainly used. With the  $k$ -point set, the surface energy converged at less than 10 meV/(1 × 1). Depending on the surface periodicity, we also used denser  $k$  points with the  $8 \times 4$ ,  $8 \times 6$ ,  $6 \times 6$ , and  $12 \times 4$  meshes in the  $1 \times 1$  surface Brillouin zone.

Within the thermodynamically allowed ranges of the Ga and Zn chemical potentials,  $\mu_{\text{Ga(bulk)}} - \Delta H_{\text{GaN}} < \mu_{\text{Ga}} < \mu_{\text{Ga(bulk)}}$  and  $\mu_{\text{Zn(bulk)}} - \Delta H_{\text{ZnO}} < \mu_{\text{Zn}} < \mu_{\text{Zn(bulk)}}$ , the surface energies with respect to the unreconstructed surface were calculated. The heat of formation for  $\Delta H_{\text{GaN}}$  is calculated to be 1.02 eV and for  $\Delta H_{\text{ZnO}}$  is 3.06 eV, which are close to the experimental results, 1.1 and 3.6 eV, respectively.<sup>28,29</sup>

### III. RESULTS

#### A. GaN(10 $\bar{1}$ 1) surface

The unreconstructed GaN(10 $\bar{1}$ 1) surface structure is shown in Fig. 1(a). The GaN(10 $\bar{1}$ 1) surface is the N-terminated semipolar surface and consists of one threefold-coordinated N (N1) and one twofold-coordinated N (N2) in an  $1 \times 1$  unit cell. In GaN, N gets 0.75 electrons per a Ga-N bond from Ga to get a total of three electrons. Thus, we consider the threefold-coordinated N1 atom to have 0.75 holes

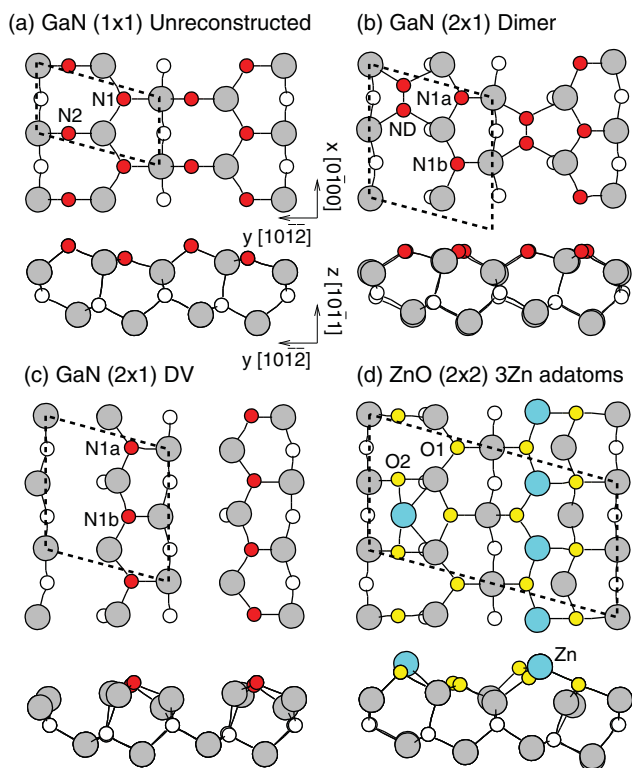


FIG. 1. (Color online) Atomic structures of the (a)  $1 \times 1$  unreconstructed, (b)  $2 \times 1$  dimerized, and (c)  $2 \times 1$  DV reconstructed GaN(10 $\bar{1}$ 1) surfaces. (d) Atomic structure of the  $2 \times 2$  3Zn adatom reconstruction of the ZnO(10 $\bar{1}$ 1) surface. The dashed lines indicate the unit cells. Large circles represent the cations and small circles the anions.

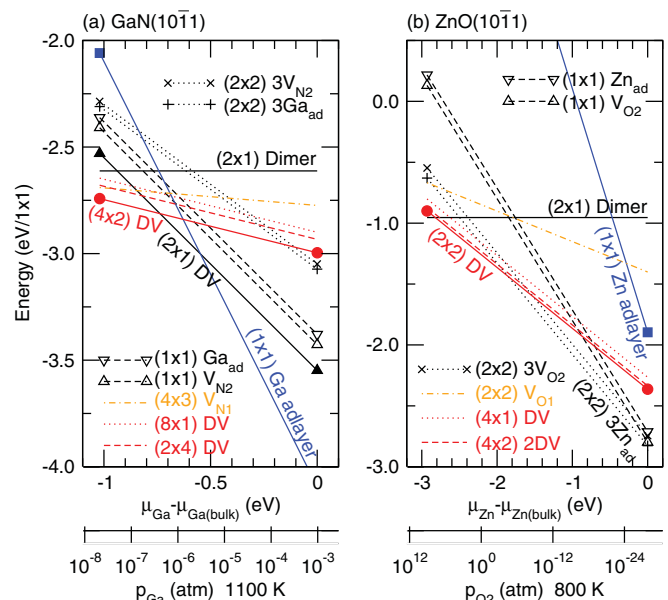


FIG. 2. (Color online) Relative energies of the reconstructed (a) GaN and (b) ZnO(10 $\bar{1}$ 1) surfaces with respect to the unreconstructed surfaces, as a function of the cation chemical potential. The relevant experimental conditions of the Ga and O<sub>2</sub> partial pressures for GaN (1100 K) [22] and ZnO (800 K) [30] respectively are shown at the bottom of each figure.

and the twofold-coordinated N2 atom to have 1.5 holes. Then, the total number of holes on the unreconstructed surface is 2.25 in an  $1 \times 1$  unit cell. The twofold-coordinated N2 atoms are Peierls unstable and prefer to form N dimers (ND). The  $1 \times 1$  periodicity of the unreconstructed surface is doubled along the dimer-bond ( $x$ ) direction. The minimum periodicity of the surface is then  $2 \times 1$ . Figure 1(b) shows the  $2 \times 1$  ND reconstruction structure. The surface energy relative to the unreconstructed surface is calculated in DFT and shown in Fig. 2(a). The  $2 \times 1$  ND structure is found to be 2.6 eV/(1 × 1) more stable than the unreconstructed surface.

Figures 3(a) and 3(b) show the calculated local density of states (LDOS) of the unreconstructed and  $2 \times 1$  ND reconstructed GaN(10 $\bar{1}$ 1) surfaces, respectively. The calculated GaN bulk band gap is 1.75 eV in the generalized gradient approximation (GGA). While on the unreconstructed surface, the Fermi level crosses the mixed N1 and N2 bands; on the  $2 \times 1$  ND reconstructed surface, the N1 band is completely filled below the Fermi level; and the ND band characterized by  $p_y p_y \pi^*$  is partially (1.5 electrons) filled inside the band gap. The ND-related  $p_z p_z \pi^*$  band is empty near the bulk conduction band maximum (CBM), and the  $p_x p_x \sigma^*$  band is found well above the CBM. Those two empty ND bands cannot act as electron-trapping states. Thus, one ND formation effectively dopes four electrons onto the unreconstructed surface, and the number of holes on the ND reconstructed surface becomes 0.5 per  $2 \times 1$ , while it is 4.5 per  $2 \times 1$  on the unreconstructed surface. The N1 atoms are threefold-coordinated with one lone pair orbital (completely filled) per atom. The N2 atoms in the dimer form are also threefold-coordinated, and the ND bond is an approximately double bond with 1.5 electrons (0.5 holes) filling the antibonding  $p_y p_y \pi^*$  state.

Since the  $2 \times 1$  ND reconstructed surface has 0.5 holes per  $2 \times 1$ , it is expected to be more stabilized by accompanying N vacancies or Ga adatoms through additional electron doping on the surface. For complete compensation, the density of N1 vacancies should be one (giving *three* electrons) per six  $2 \times 1$  unit cells, preserving the N2-dimer density. For N2 vacancies, in order to avoid a single nondimerized N2 atom, the N2 vacancies should be paired along the dimer-row ( $x$ ) direction, so that all the other N2 atoms are dimerized. Two N2 vacancies (providing six electrons) remove one ND (generating four holes), and then effectively two N2 vacancies dope *two* electrons on the ND reconstructed surface. The separated two N2 vacancies are found to be less stable than the neighboring two N2 vacancies (DV). A Ga adatom (giving three electrons) is located between two N2 atoms as a bridge configuration [likely shown in Fig. 1(d)] and removes one ND bond (generating four holes). Then, effectively the Ga adatom dopes *one hole* on the ND reconstructed surface, and thus the Ga adatom does not act as an electron donor on the ND reconstructed GaN( $10\bar{1}1$ ) surface. The number of holes on the dimerized GaN( $10\bar{1}1$ ) surface is then simply calculated from Eq. (1):

$$h = \frac{1}{2} - \frac{3N(V_{N1}) + 2N(DV) - 1N(Ga_{ad})}{n}, \quad (1)$$

where  $h$  is the hole density in  $2 \times 1$ , and  $N(V_{N1})$ ,  $N(DV)$ , and  $N(Ga_{ad})$  are the number of N1 vacancies, DV, and Ga adatoms, respectively, in  $n$  times  $2 \times 1$  unit cells.

We calculated N1-vacancy-involved ND reconstructions for  $n = 6$  and  $N(V_{N1}) = 1$  in  $12 \times 1$ ,  $2 \times 6$ ,  $6 \times 2$ , and  $4 \times 3$

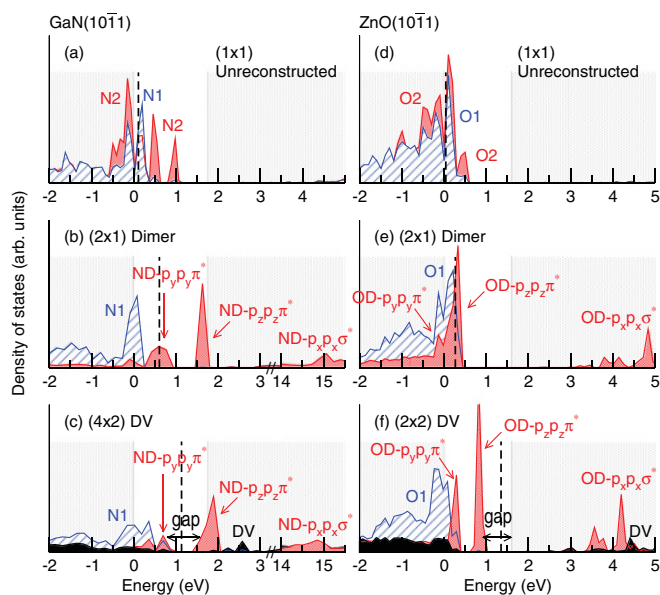


FIG. 3. (Color online) LDOS of the (a)  $1 \times 1$  unreconstructed, (b)  $2 \times 1$  dimer, and (c)  $4 \times 2$  DV reconstructed GaN( $10\bar{1}1$ ) surfaces. LDOS of the (d)  $1 \times 1$  unreconstructed, (e)  $2 \times 1$  dimer, and (f)  $2 \times 2$  DV reconstructed ZnO( $10\bar{1}1$ ) surfaces. The (blue) line-filled area is for the N1(O1) atoms, the (red) half-filled area is for the N2(O2) or ND(OD) atoms, and the (black) completely filled area is for the Ga(Zn) atoms near DV on the GaN(ZnO) surface. The bulk valance and conduction bands are indicated by (gray) dotted area, and the Fermi level is given by the (black) vertical dashed lines.

periodicities in DFT. The N1-vacancy-involved ND reconstructed GaN( $10\bar{1}1$ ) surface is more stable than that without vacancy, as shown in Fig. 2(a) (representatively for  $4 \times 3$ ), making the surface semiconducting and satisfying the electron counting rule. On the other hand, the N2-vacancy-involved structure is found to be more stable than the N1-vacancy-involved structure. A N2-vacancy leaves only two nearby threefold Ga atoms, while a N1-vacancy leaves three threefold Ga atoms. The N2-vacancy-involved ND reconstructed surface is calculated for  $n = 4$  and  $N(DV) = 1$  by putting two N2 vacancies in  $4 \times 2$ ,  $2 \times 4$ , and  $8 \times 1$  unit cells. The  $4 \times 2$  DV reconstructed surface is found to be the most stable, as shown in Fig. 2(a).

The stability of the  $4 \times 2$  DV reconstruction with respect to the  $2 \times 4$  and  $8 \times 1$  reconstructions can be understood by electrostatics. The DVs in the  $4 \times 2$  DV reconstruction are arranged in a two-dimensional oblique (parallelogrammic) lattice [Fig. 4(a)], while an entire dimer row along the  $x$  axis is missing every four dimer rows in the  $2 \times 4$  DV reconstruction [Fig. 4(b)] and the DVs are arranged across the dimer rows in

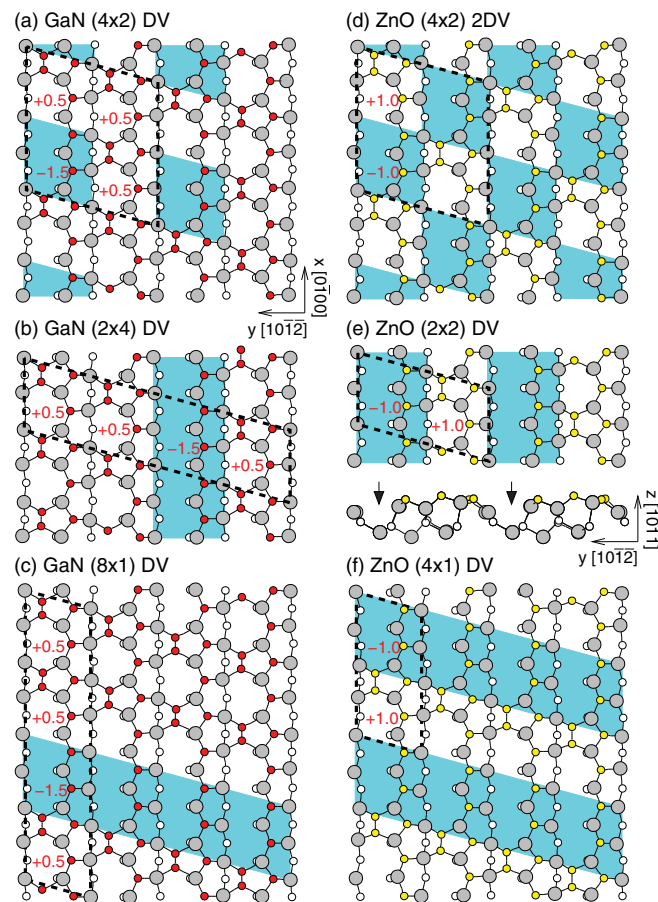


FIG. 4. (Color online) Atomic structures of the (a)  $4 \times 2$ , (b)  $2 \times 4$ , and (c)  $8 \times 1$  DV reconstructions of the GaN( $10\bar{1}1$ ) surface and of the (d)  $4 \times 2$  2DV, (e)  $2 \times 2$ , and (f)  $4 \times 1$  DV reconstructions of the ZnO( $10\bar{1}1$ ) surface. The side view of the  $2 \times 2$  DV reconstruction is also shown in (e). The dashed lines indicate the unit cells, and the (cyan) shaded areas are the cells where the DVs are located. In (e), dips on the surface are indicated by arrows.

the  $8 \times 1$  DV reconstruction [Fig. 4(c)]. Since a DV-involved  $2 \times 1$  cell donates 1.5 electrons and a ND-included  $2 \times 1$  cell gains 0.5 electrons, we can compare the electrostatic (Madelung) energies. With respect to the most stable  $4 \times 2$  DV reconstruction, the calculated electrostatic energies ( $\epsilon_{\text{GaN}} = 9.7$ ) of the  $2 \times 4$  and  $8 \times 1$  DV reconstructions are 0.254 and 0.301 eV/( $1 \times 1$ ), respectively, which are similar in the stability order with the DFT results of respectively 0.063 and 0.096 eV/( $1 \times 1$ ) [Fig. 2(a)]. The other DV-involved reconstruction structures, such as segregated DVs in a cell larger than four times  $2 \times 1$ , can be excluded based on this argument.

In Fig. 2(a), we compare the DFT surface energies of various GaN( $10\bar{1}1$ ) surface reconstruction structures, including the previously suggested ones. The  $1 \times 1$  Ga-adatom<sup>21</sup> and  $1 \times 1$  N2-vacancy<sup>22</sup> structures, which have 0.75 electrons per  $1 \times 1$ , are respectively 0.38 and 0.33 eV/( $1 \times 1$ ) higher in surface energy than the  $4 \times 2$  DV structure in the N-rich limit condition. The  $4 \times 2$  DV structure is the most stable in  $-1.0 \text{ eV} < \mu_{\text{Ga}} - \mu_{\text{Ga}(\text{bulk})} < -0.7 \text{ eV}$ . On the GaN( $10\bar{1}1$ ) Ga semipolar surface, a similar DV reconstruction with the  $2 \times 2$  periodicity has been suggested in N-rich limit conditions.<sup>31</sup> As the  $\mu_{\text{Ga}}$  increases, the  $2 \times 1$  DV structure [Fig. 1(c)] is stabilized [ $-0.7 \text{ eV} < \mu_{\text{Ga}} - \mu_{\text{Ga}(\text{bulk})} < -0.5 \text{ eV}$ ]. In this structure, all the N2 surface atoms are removed, and the surface is  $n$  type with the charge density of  $-1.5$  per  $2 \times 1$ . The periodicity doubling from the  $1 \times 1$  N2-vacancy structure occurs by Peierls instability of the N2 vacancies (threefold Ga atoms) arranged along the  $x$  axis. In Ga-rich conditions [ $-0.5 \text{ eV} < \mu_{\text{Ga}} - \mu_{\text{Ga}(\text{bulk})} < 0.0 \text{ eV}$ ], the well-known  $1 \times 1$  Ga-adlayer structure is the most stable, as in the previous results.<sup>14,15,21,22</sup>

### B. ZnO( $10\bar{1}1$ ) surface

For the ZnO( $10\bar{1}1$ ) surface, we can apply the same argument, but the electron counting numbers are different. In ZnO, O gets 0.5 electrons per Zn-O bond. The number of holes on the unreconstructed surface is 1.5 in  $1 \times 1$ . The surface twofold-coordinated O2 atoms form O dimers (OD), and the  $2 \times 1$  dimerized surface is found to be 0.95 eV/( $1 \times 1$ ) more stable than the unreconstructed surface [Fig. 2(b)]. The OD bonding is weaker than the ND bonding. The LDOS of the  $2 \times 1$  OD reconstructed structure is shown in Fig. 3(e). The calculated ZnO bulk band gap is 1.59 eV in the GGA +  $U$ . The  $p_y p_y \pi^*$  is completely filled, and the  $p_z p_z \pi^*$  is partially (half) filled inside the band gap. The  $p_x p_x \sigma^*$  band is well above the CBM and completely empty. The one empty  $p_x p_x \sigma^*$  band cannot trap electrons, and thus one OD formation dopes *two* electrons onto the unreconstructed surface. The number of holes on the OD reconstructed surface is 1.0 per  $2 \times 1$ , while it is 3.0 per  $2 \times 1$  on the unreconstructed surface.

An O1 vacancy dopes *two* electrons, and a Zn adatom in a bridge configuration [as shown in Fig. 1(d)] does not dope charges onto the OD reconstructed surface (a Zn adatom gives two electrons, and removal of an OD bonding generates two holes). Two O2 vacancies dope *two* electrons (two O2 vacancies give four electrons, and removal of an OD generates two holes). The number of holes on the dimerized ZnO( $10\bar{1}1$ )

surface can be calculated from Eq. (2):

$$h = 1 - \frac{2N(V_{\text{O}1}) + 2N(\text{DV}) + 0N(\text{Zn}_{\text{ad}})}{n}, \quad (2)$$

where  $h$  is the hole density in  $2 \times 1$ , and the  $N(V_{\text{O}1})$ ,  $N(\text{DV})$ , and  $N(\text{Zn}_{\text{ad}})$  are the number of O1 vacancies, DV, and Zn adatoms, respectively, in  $n$  times  $2 \times 1$  unit cells.

The calculated DFT surface energies of ZnO( $10\bar{1}1$ ) are compared in Fig. 2(b). In order to compensate the 1.0 hole per  $2 \times 1$  on the dimerized surface, the O1-vacancy-involved [ $n = 2$  and  $N(V_{\text{O}1}) = 1$  in  $2 \times 2$  and  $4 \times 1$ ] and O2-vacancy-involved [ $n = 2$  and  $N(\text{DV}) = 1$  in  $2 \times 2$  and  $4 \times 1$ , and  $n = 4$  and  $N(\text{DV}) = 2$  in  $4 \times 2$ ] OD reconstructions are considered. The  $2 \times 2$  DV reconstruction is found to be the most stable in O-rich conditions [ $-3.0 \text{ eV} < \mu_{\text{Zn}} - \mu_{\text{Zn}(\text{bulk})} < -1.8 \text{ eV}$ ]. The  $4 \times 2$  2DV and  $4 \times 1$  DV reconstructions are 0.028 and 0.099 eV/( $1 \times 1$ ) higher in DFT surface energy than the  $2 \times 2$  DV, respectively [Fig. 2(b)]. In the  $2 \times 2$  DV reconstruction, a dimer row is missing every two dimer rows [Fig. 4(e)]. In contrast to the GaN( $10\bar{1}1$ ) surface, where the oblique lattice of the  $4 \times 2$  DV is stable, the  $4 \times 2$  2DV reconstruction of such a lattice [Fig. 4(d)] is found to be less stable in DFT than the  $2 \times 2$  DV [Fig. 4(e)]. The calculated Madelung energies ( $\epsilon_{\text{ZnO}} = 8.65$ ) of the  $4 \times 2$  2DV and  $4 \times 1$  DV are  $-0.040$  and  $+0.019 \text{ eV}/(1 \times 1)$  with respect to the  $2 \times 2$  DV, respectively. It might be due to the small electrostatic energy difference for ZnO( $10\bar{1}1$ ) and the electronic binding contribution of the ODs along the dimer row through the occupied  $p_z p_z \pi^*$  channel. The  $2 \times 2$  DV structure is consistent with the TEM experiment that observed  $a \times 2$  reconstruction with *dips* every two unit cells along the  $y$  axis.<sup>23</sup> The dips are suggested here to be the missing dimer rows in the  $2 \times 2$  DV reconstruction, as shown in Fig. 4(e). In  $-1.8 \text{ eV} < \mu_{\text{Zn}} - \mu_{\text{Zn}(\text{bulk})} < 0.0 \text{ eV}$ , the  $2 \times 2$  3Zn adatom structure [Fig. 1(d)] is found to be the most stable [Fig. 2(b)], which satisfies the electron counting rule without ODs (the six holes in  $2 \times 2$  on the unreconstructed surface are compensated by the Zn adatoms, not by ODs), and is semiconducting. The Zn-adlayer metallic reconstruction is not found to be stable even in Zn-rich conditions, unlike the GaN( $10\bar{1}1$ ) surface.

## IV. CONCLUSION

In conclusion, we have suggested the semiconducting reconstruction structures of the GaN and ZnO( $10\bar{1}1$ ) surfaces. The  $4 \times 2$  DV reconstruction on the GaN( $10\bar{1}1$ ) surface is found to be the lowest in surface energy in N-rich conditions among the considered structures, including the previously suggested ones, and is proposed to be the ground-state configuration based on the electrostatics and DFT. The  $2 \times 2$  DV reconstruction on the ZnO( $10\bar{1}1$ ) surface is found to be the most stable in O-rich conditions in DFT and explains the measured  $2 \times a$  reconstruction structure with the regularly arranged dips.

## ACKNOWLEDGMENTS

This work is supported by the Nano Research and Development program through the National Research Foundation of Korea funded by the Ministry of Education, Science, and Technology (No. 2009-0082489).

\*yongsung.kim@kriss.re.kr

- <sup>1</sup>P. Waltereit, O. Brandt, A. Trampert, H. T. Grahn, J. Menniger, M. Ramsteiner, M. Reiche, and K. H. Ploog, *Nature (London)* **406**, 865 (2000).
- <sup>2</sup>T. Hikosaka, T. Narita, Y. Honda, M. Yamaguchi, and N. Sawaki, *Appl. Phys. Lett.* **84**, 4717 (2004).
- <sup>3</sup>M. Ueda, K. Kojima, M. Funato, Y. Kawakami, Y. Narukawa, and T. Mukai, *Appl. Phys. Lett.* **89**, 211907 (2006).
- <sup>4</sup>G.-T. Chen, S.-P. Chang, J.-I. Chyi, and M.-N. Chang, *Appl. Phys. Lett.* **92**, 241904 (2008).
- <sup>5</sup>S. Schwaiger, I. Argut, T. Wunderer, R. Rösch, F. Lipski, J. Biskupek, U. Kaiser, and F. Scholz, *Appl. Phys. Lett.* **96**, 231905 (2010).
- <sup>6</sup>H. Li, A. H. Chin, and M. K. Sunkara, *Adv. Mater.* **18**, 216 (2006).
- <sup>7</sup>X. M. Cai, A. B. Djurišić, M. H. Xie, C. S. Chiu, and S. Gwo, *Appl. Phys. Lett.* **87**, 183103 (2005).
- <sup>8</sup>S. Kitamura, K. Hiramatsu, and N. Sawaki, *Jpn. J. Appl. Phys.* **34**, L1184 (1995).
- <sup>9</sup>C. Liu, P. A. Shields, Q. Chen, D. W. E. Allsopp, W. N. Wang, C. R. Bowen, T.-L. Phan, and D. Cherns, *Phys. Status Solidi C* **7**, 32 (2010).
- <sup>10</sup>S. M. de S. Pereira, M. A. Martins, T. Trindade, I. M. Watson, D. Zhu, and C. J. Humphreys, *Adv. Mater.* **20**, 1038 (2008).
- <sup>11</sup>L. Zhou, M. R. McCartney, D. J. Smith, A. Mouti, E. Feltin, J. F. Carlin, and N. Grandjean, *Appl. Phys. Lett.* **97**, 161902 (2010).
- <sup>12</sup>W. Harrison, *J. Vac. Sci. Technol.* **16**, 1492 (1979).
- <sup>13</sup>S. B. Zhang and S.-H. Wei, *Phys. Rev. Lett.* **92**, 086102 (2004).
- <sup>14</sup>J. Neugebauer, *Phys. Status Solidi B* **227**, 93 (2001).
- <sup>15</sup>A. R. Smith, R. M. Feenstra, D. W. Greve, J. Neugebauer, and J. E. Northrup, *Phys. Rev. Lett.* **79**, 3934 (1997).
- <sup>16</sup>K. Rapcewicz, M. Buongiorno Nardelli, and J. Bernholc, *Phys. Rev. B* **56**, R12725 (1997).
- <sup>17</sup>J. Elsner, M. Haugk, G. Jungnickel, and Th. Frauenheim, *Solid State Commun.* **106**, 739 (1998).
- <sup>18</sup>Q.-K. Xue, Q. Z. Xue, R. Z. Baktizin, Y. Hasegawa, I. S. T. Tsong, T. Sakurai, and T. Ohno, *Phys. Rev. Lett.* **82**, 3074 (1999).
- <sup>19</sup>J. E. Northrup, J. Neugebauer, R. M. Feenstra, and A. R. Smith, *Phys. Rev. B* **61**, 9932 (2000).
- <sup>20</sup>F.-H. Wang, P. Krüger, and J. Pollmann, *Phys. Rev. B* **64**, 035305 (2001).
- <sup>21</sup>J. E. Northrup, L. T. Romano, and J. Neugebauer, *Appl. Phys. Lett.* **74**, 2319 (1999).
- <sup>22</sup>T. Akiyama, D. Ammi, K. Nakamura, and T. Ito, *Phys. Rev. B* **81**, 245317 (2010).
- <sup>23</sup>Y. Ding and Z. L. Wang, *Surf. Sci.* **601**, 425 (2007).
- <sup>24</sup>G. Kresse and D. Joubert, *Phys. Rev. B* **59**, 1758 (1999).
- <sup>25</sup>P. E. Blöchl, *Phys. Rev. B* **50**, 17953 (1994).
- <sup>26</sup>J. P. Perdew and Y. Wang, *Phys. Rev. B* **45**, 13244 (1992).
- <sup>27</sup>V. I. Anisimov, I. V. Solovyev, M. A. Korotin, M. T. Czyżyk, and G. A. Sawatzky, *Phys. Rev. B* **48**, 16929 (1993).
- <sup>28</sup>H. Hahn and R. Juza, *Z. Anorg. Chem.* **244**, 111 (1940).
- <sup>29</sup>J. A. Dean, *Lange's Handbook of Chemistry*, 14th ed. (McGraw-Hill, New York, 1992).
- <sup>30</sup>K. Reuter and M. Scheffler, *Phys. Rev. B* **65**, 035406 (2001).
- <sup>31</sup>T. Akiyama, D. Ammi, K. Nakamura, and T. Ito, *Jpn. J. Appl. Phys.* **48**, 100201 (2009).